Journal of Electroceramics 6:1, 61–74, 2001

Thermoelectricity of $BaTiO_{3+\delta}$

HAN-ILL YOO* & CHANG-ROCK SONG¶

Solid State Ionics Research Laboratory, School of Materials Science and Engineering, Seoul National University, Seoul 151–742, Korea

Submitted July 18, 2000; Revised October 18, 2000; Accepted October 19, 2000

Abstract. Thermoelectricity of mixed ionic electronic conductor $BaTiO_{3+\delta}$ is thermodynamically analyzed, and measured across the mixed n/p regime of both undoped and 1.8 m/o A1-doped $BaTiO_3$ at elevated temperatures. There can be 4 different measurement conditions with respect to the nonstoichiometry (δ) redistribution and types of atmosphere gases used to control the surrounding oxygen potential, which lead to differences in information content of the thermopower. Experimental thermopower isotherms are exhaustively analyzed to find that the ionic contribution is evident in the mixed n/p regime and that the heats of transport of electrons and holes are about the same as their migration enthalpies.

Keywords: $BaTiO_3$, thermopower, heat of transport, mixed ionic electronic conductor.

1. Introduction

$BaTiO_{3+\delta}$ is a very interesting oxide not only from a practical point of view, but also from a defect chemical point of view. The oxide is a mixed ionic electronic conductor (MIEC) in a quite extended range of oxygen partial pressure (e.g., $-15 \leq \log (Po_2/atm) \leq 0$ at 1000°C), in the middle of which a p-type to n-type transition occurs, while the ionic partial conductivity remains nearly independent of Po_2 [1]. This sort of electron/hole/ion mixed conduction is quite rare in binary oxides. MnO and TiO_2, among others, are reported to show a mixed n/p behavior [2–4], but these oxides are nearly totally electronic so any ionic contribution is hardly seen and either the n-type (for MnO) or p-type (for TiO_2) regime of Po_2 is so narrow that precise observation of even the n/p mixed behavior is often prone to experimental difficulty.

For the system of $BaTiO_3$, the total electrical conductivity has been extensively documented against temperature and oxygen partial pressure, and the working model of its defect structure is available [5,6]. We have recently reported on the chemical diffusivity as a measure of (oxygen) nonstoichiometry re-equilibration kinetics for "undoped" and 1.8 m/o A1-doped $BaTiO_3$, respectively [7–11]. From the electrical conductivity and diffusivity combined, the mobilities of electrons and holes have first been separately evaluated along with the other defect chemical parameters, including the intrinsic electronic excitation equilibrium constant [7,9,11], and in turn, the oxygen nonstoichiometry was also evaluated [12].

As a sequel to the previous works on $BaTiO_3$ [7–11], the present work is concerned with its thermoelectric behavior. The thermoelectric power has earlier been reported on the same and similar systems [6, 13–17] but mostly to identify the types of electronic carriers [13] or to estimate the electronic carrier densities [16,14–17]. As is well known [18], the thermopower of an MIEC, $BaTiO_3$ is a combination of the ionic and electronic contributions, and each is mostly determined by the partial molar entropy and heat of transport of the respective carriers. To date, the heat of transport has not been so well understood theoretically or experimentally [19]. It is thus not straightforward to evaluate the electronic carrier densities of $BaTiO_3$ from its overall thermopower, without paying due attention to the heats of transport of electrons and holes, as well as to the ionic contribution.

In this paper, we will analyze thermodynamically

*Author to whom all correspondence should be addressed.
¶Now with Hyundai Electronics Co., Ltd., Ichon, Kyoungki-Do, 467–701, Korea.

and experimentally the thermoelectricity of $BaTiO_{3+\delta}$ as a model of MIEC oxides with both ionic carriers and electronic carriers of electrons and holes.

2. Thermodynamic Analysis

The general, irreversible thermodynamic treatment of the thermoelectric power of mixed ionic electronic conductor compounds has earlier been given by Wagner [18], and particularly for electrolytic oxides by Yoo and Hwang [20]. With $BaTiO_3$ specifically in mind, we will here deal with an MIEC with only one type of ionic carriers, say, oxide anions (O^{2-}) and electron and holes as electronic carriers. Nevertheless, the treatment given here can be readily generalized with minor modifications. (The reader should consult the "List of Symbols" at the end of the paper for definitions of symbols used in the equations.)

The absolute thermopower of $BaTiO_3$ can be determined by adding to the thermopower θ_{Cell} as measured from a thermocell,

$$\underset{T}{Pt, P_{O_2}} \left| \underset{T}{BaTiO_3} \right| \underset{T+\Delta T}{P_{O_2}, Pt} \qquad (I)$$

the absolute thermopower of lead wire Pt, θ_{Pt} or

$$\theta = \theta_{Cell} + \theta_{Pt}. \qquad (1)$$

In accord with Wagner, [18] the thermopower is defined here as

$$\theta \equiv \lim_{\Delta T \to 0} \frac{\Delta \phi}{\Delta T} = -\frac{1}{e}\frac{d\eta_{el}}{dT} \qquad (2)$$

This definition leads to a positive sign of the thermopower of a normal n-type semiconductor. (The opposite sign convention is normally employed in semiconductor literatures) [21, 22].

For $BaTiO_3$, one may take oxide anions (O^{2-}) and electrons (e^-) as the mobile charged components as the rest of the cations are practically immobile [5,9]. In a non-isothermal condition, a current by each of these components arises as

$$i_k = -\frac{\sigma_k}{z_k e}\left[\nabla\eta_k + \left(\bar{S}_k + \frac{q_k^*}{T}\right)\nabla T\right], \quad [k = ion(=O^{2-}), el(=e^-)]. \qquad (3)$$

Due to the open-circuit condition, $i_{ion} + i_{el} = 0$, or through an equivalent circuit analysis [23], one may solve for the gradient of electronic electrochemical potential $\nabla\eta_{el}$ to obtain via Eq. (2)

$$\theta = t_{el}\theta_{el} + t_{ion}\theta_{ion} \qquad (4)$$

$$= \frac{t_{el}}{e}\left(\bar{S}_{e^-} + \frac{q_{e^-}^*}{T}\right) + \frac{t_{ion}}{ze}\left(\frac{d\mu_o}{dT} + \bar{S}_{O^{2-}} + \frac{q_{O^{2-}}^*}{T}\right) \qquad (4a)$$

where we have employed the ionization reaction equilibrium of the neutral component oxygen (O) in $BaTiO_3$,

$$\nabla\eta_{O^{2-}} = \nabla\mu_O + 2\nabla\eta_{el}. \qquad (5)$$

Electronic Contribution

The thermopower, θ_{el}, in Eq. (4a) represents the contribution by electrons as a charged component. The latter may be equivalently expressed in terms of the contributions by two types of electronic carriers, electrons and holes as follows. For each of electrons and holes, one can write a flux equation similar to Eq. (3) and combine them via the relation $i_n + i_p = 0$ or equivalent circuit analysis to obtain

$$\theta_{el} = \frac{1}{e}\left[\frac{\sigma_n}{\sigma_n + \sigma_p}\left(\bar{S}_n + \frac{q_n^*}{T}\right) - \frac{\sigma_p}{\sigma_n + \sigma_p}\left(\bar{S}_p + \frac{q_n^*}{T}\right)\right] \qquad (6)$$

where the quantities corresponding to electrons and holes are denoted by subscripts n and p, respectively. Here, use was made of the identity

$$\eta_n + \eta_p = \mu_n + \mu_p = 0. \qquad (7)$$

This identity leads to the relation

$$T(\bar{S}_n + \bar{S}_p) = \bar{H}_n + \bar{H}_p = \Delta H_i \qquad (8)$$

where ΔH_i corresponds to the thermal band gap of $BaTiO_3$. [See Eq. (17) below. This is identical to Eq. (7) in association with Eq. (9).]

One may assume the Boltzmann approximation for electrons and holes, as is the case with $BaTiO_3$, [18]

$$\bar{S}_n = \bar{S}_n^o - k\ln n \;;\; \bar{S}_p = \bar{S}_p^o - k\ln p \qquad (9)$$

to rewrite Eq. (6), after some algebra, as

$$\theta_{el} = \frac{1}{2e}\left[\frac{\Delta H_i + q_n^* + q_p^*}{T}\tanh\left(\frac{1}{2}\ln a\right) - k\ln(ab) - \left(\bar{S}_n^o - \bar{S}_p^o + \frac{q_n^* - q_p^*}{T}\right)\right] \quad (10)$$

where a and b are defined as the conductivity and mobility ratio, respectively, or

$$a \equiv \frac{\sigma_p}{\sigma_n} = \frac{p}{nb} \quad ; \quad b \equiv \frac{u_n}{u_p} \quad (11)$$

This is essentially identical to what has earlier been derived by Wagner [18] in the light of irreversible thermodynamics and by Frederickse [21] and Jonker [22] in the light of semiconductor physics.

Ionic Contribution

As is seen in Eq. (4a), the ionic thermopower, θ_{ion}, involves a term which has no analogue in the electronic thermopower, that is,

$$\frac{d\mu_O}{dT} = \left(\frac{\partial \mu_O}{\partial T}\right)_\delta + \left(\frac{\partial \mu_O}{\partial \delta}\right)_T \frac{d\delta}{dT} = -\bar{S}_O + W \quad (12)$$

as the chemical potential of neutral oxygen, μ_o, is a function of T and δ for the system of $Ba_{1+\xi}TiO_{3+\delta}$, assuming that the cation composition or non-molecularity (ξ) remains homogeneously fixed. The very term, $d\mu_o/dT$, takes different values depending on the measurement conditions. The first term on the right hand side of the first identity, is just the partial molar entropy of component oxygen $\mathbf{S_O}$ in $BaTiO_3$, which depends on gas atmospheres in the surroundings, assuming gas/solid oxygen exchange equilibrium prevailing. The oxygen partial pressure in the surroundings is normally controlled by O_2/inert gas (e.g., N_2) mixtures and/or CO_2/CO gas mixtures. In the former, Po_2 is fixed and in the latter the mixing ratio $r(= P_{CO_2}/P_{CO})$ is fixed. Thus,

1) In O_2/N_2 atmospheres,

$$-\bar{S}_o = -\frac{1}{2}S^o_{O_2(g)} + \frac{1}{2}k\ln P_{O_2} \quad (13)$$

due to

$$\mu_O = \frac{1}{2}\mu_{O_2(g)} \quad (14)$$

2) In CO_2/CO atmospheres,

$$-\bar{S}_O = -S^o_{CO_2} + S^o_{CO} + k\ln r = -\frac{1}{2}S^o_{O_2} - \frac{\Delta H^o_g}{T} + \frac{1}{2}k\ln P_{O_2} \quad (15)$$

due to the reaction equilibrium $CO + \frac{1}{2}O_2 = CO_2$ or

$$\mu_O = \frac{1}{2}\mu_{O_2(g)} = \mu_{CO_2} - \mu_{CO} \quad (16)$$

where ΔH^o_g is the standard enthalpy of the reaction.

The factor W in Eq. (12) will depend on whether the thermopower is determined at a uniform distribution of nonstoichiometry ($\nabla\delta = 0$) or under a steady state, non-zero gradient ($\nabla\delta \neq 0$) [18,20]. The latter condition may further enclose two possibilities: one is the Soret equilibrium [18,20,24] and the other the steady state in equilibrium with the immediate local surroundings (T, Po_2). The Soret equilibrium can only be achieved when the system is completely closed, but this closed condition is not so easy to realize experimentally with an oxide in particular. The second condition is the most viable experimentally if the system is left open and the nonstoichiometry equilibration kinetics is fast enough. $BaTiO_3$, of present concern, is such a case [7–11]. We will thus evaluate the W-factor for this possibility. For the case of Soret equilibrium, the readers are referred to Refs. [18] and [20].

In order to explicitly evaluate the factor W, one should invoke the defect structure of the system of concern. The defect structure of the system of $BaTiO_{3+\delta}$ can be satisfactorily described by the two defect equilibria [9,11],

$$0 = e' + h^\cdot \quad ; \quad K_i = np = K_{i,0}\exp\left(-\frac{\Delta H_i}{kT}\right) \quad (17)$$

$$O_O^x = V_O^{\bullet\bullet} + 2e' + \frac{1}{2}O_2 \quad ;$$
$$K_R = [V_O^{\bullet\bullet}]n^2 a_{O_2}^{1/2} = K_{R,0}\exp\left(-\frac{\Delta H_R}{kT}\right) \quad (18)$$

and the charge neutrality condition,

$$n + 2[V_O^{\bullet\bullet}] = p + [A_C'] \quad (19)$$

where A_C' stands for the effective acceptors on the cation sites that may be either (background or intentionally doped) impurity acceptors or cation vacancies [9]. In the n/p mixed regime of our major concern, where the majority type of defects are $2[V_O^{\cdot\cdot}] \approx [A_C']$, [9,11] the oxygen nonstoichiometry is given as [8–11]

$$\delta = \frac{V_m}{N_A}\sqrt{K_i}\sinh\left(\frac{1}{4}\ln\frac{a_{O_2}}{a^o_{O_2}}\right) \;;$$
$$a^o_{O_2} = \frac{4}{[A'_C]^2}\left(\frac{K_R}{K_i}\right)^2 \qquad (20)$$

where $a^o_{O_2}$ denotes the oxygen activity (= Po_2/atm) for the electronic stoichiometric composition or n = p.

Therefore, the factor W takes the values depending on the measurement conditions:

1) When $\nabla\delta = 0$, in any atmosphere

$$W = 0. \qquad (21)$$

2) When $\nabla\delta \neq 0$ in Po_2 = fixed (N_2/O_2) atmospheres, due to Eq. (20),

$$W = \frac{\Delta H_i}{T}\tanh\left(\frac{1}{4}\ln\frac{a_{O_2}}{a^o_{O_2}}\right) - \frac{\Delta H_R - \Delta H_i}{T} \qquad (22)$$

3) When $\nabla\delta \neq 0$ in r = fixed (CO_2/CO) atmospheres, due to Eqs. (20) and (16),

$$W = \frac{\Delta H_i}{T}\tanh\left(\frac{1}{4}\ln\frac{a_{O_2}}{a^o_{O_2}}\right) - \frac{\Delta H_R - \Delta H_i + \Delta H^o_g}{T} \qquad (23)$$

There can, thus, be 4 possible experimental combinations of thermopower measurement among the two atmosphere control methods (O_2/N_2 and CO_2/CO) and the two nonstoichiometry distribution conditions ($\nabla\delta = 0$ and $\nabla\delta \neq 0$). Concordantly, the ionic thermopower takes the forms, respectively:

(1) When $\nabla\delta = 0$ in O_2/N_2 atmospheres,

$$\theta_{ion}(O_2/N_2;\nabla\delta = 0) = \frac{1}{2e}\left(-\frac{1}{2}S^o_{O_2} + \frac{1}{2}k\ln a_{O_2} + \bar{S}_{O^{2-}} + \frac{q^*_{O^{2-}}}{T}\right) \qquad (24)$$

(2) when $\nabla\delta \neq 0$ in O_2/N_2 atmospheres,

$$\theta_{ion}(O_2/N_2;\nabla\delta \neq 0) = \frac{1}{2e}\left\{-\frac{1}{2}S^o_{O_2} + \frac{1}{2}k\ln a_{O_2} + \bar{S}_{O^{2-}} - \frac{q^*_{O^{2-}}}{T} + \frac{\Delta H_i}{T}\left[1+\tanh\left(\frac{1}{4}\ln\frac{a_{O_2}}{a^o_{O_2}}\right)\right] - \frac{\Delta H_R}{T}\right\} \qquad (25)$$

(3) when $\nabla\delta = 0$ in CO_2/CO atmospheres,

$$\theta_{ion}(CO_2/CO;\nabla\delta = 0) = \frac{1}{2e}\left(-\frac{1}{2}S^o_{O_2} + \frac{1}{2}k\ln a_{O_2} + \bar{S}_{O^{2-}} + \frac{q^*_{O^{2-}}}{T} - \frac{\Delta H^o_g}{T}\right) \qquad (26)$$

(4) when $\nabla\delta \neq 0$ in CO_2/CO atmospheres,

$$\theta_{ion}(CO_2/CO;\nabla\delta \neq 0) = \frac{1}{2e}\left\{-\frac{1}{2}S^o_{O_2} + \frac{1}{2}k\ln a_{O_2} + \bar{S}_{O^{2-}} + \frac{q^*_{O^{2-}}}{T} + \frac{\Delta H_i}{T}\left[1+\tanh\left(\frac{1}{4}\ln\frac{a_{O_2}}{a^o_{O_2}}\right)\right] - \frac{\Delta H_R}{T} - \frac{2\Delta H^o_g}{T}\right\} \qquad (27)$$

In the defect regime $[A'_C] \approx [V^{\cdot\cdot}_O]$ of present concern, the electronic conductivity ratio and mobility ratio in Eq. (11) are given as [9–11]

$$a = \left(\frac{a_{O_2}}{a^*_{O_2}}\right)^{1/2} \;;\; b = \left(\frac{a^*_{O_2}}{a^o_{O_2}}\right)^{1/2} \qquad (28)$$

where $a^*_{O_2}$ denotes the oxygen activity at which $\sigma_n = \sigma_p$ (or at the conductivity minimum in Fig. 5 below). The electronic thermopower of Eq. (10) is thus rewritten as

$$\theta_{el} = -\frac{1}{2e}\left[\frac{\Delta H_i + q^*_n + q^*_p}{T}\tanh\left(\frac{1}{4}\ln\frac{a_{O_2}}{a^*_{O_2}}\right) - \frac{1}{2}k\ln\frac{a_{O_2}}{a^*_{O_2}} - k\ln b - \left(\bar{S}^o_n - \bar{S}^o_p + \frac{q^*_n - q^*_p}{T}\right)\right] \qquad (29)$$

The absolute thermopower of $BaTiO_{3+\delta}$ in the defect regime of $[A'_C] \approx [V^{\cdot\cdot}_O]$ can finally be evaluated by combining, via Eq. (4), Eq. (29) and one of Eqs. (24)–(27) depending on the experimental conditions. It is noted that if $t_{el} >> t_{ion}$, the thermopower will be essentially independent of the measurement conditions and anti-symmetric versus $\ln a_{O_2}$. On the other hand, once the thermopower turns out to depend on the measurement conditions, the ionic contribution will have to be appreciable.

It may be of some interest to see the difference in information content between the absolute thermopowers of $BaTiO_3$ which are to be measured in different measurement conditions.

1) Thermopowers measured in a CO_2/CO atmosphere and the corresponding O_2/N_2 atmosphere: If the thermopower is determined under the condition of $\nabla\delta = 0$, then one has, due to Eqs. (4), (10) or (29), (24), and (26),

$$\theta(O_2/N_2;\nabla\delta=0) = \theta(CO_2/CO;\nabla\delta=0) + t_{ion}\frac{\Delta H_g^o}{2eT} \tag{30}$$

For the measurement condition under a steady state distribution of nonstoichiometry or $\nabla\delta \neq 0$, one has due to Eqs. (4), (10) or (29), (25), and (27),

$$\theta(O_2/N_2;\nabla\delta\neq0) = \theta(CO_2/CO;\nabla\delta\neq0) + t_{ion}\frac{\Delta H_g^o}{eT} \tag{31}$$

2) Thermopowers measured in the state of $\nabla\delta = 0$ and of $\nabla\delta \neq 0$: The information content differs depending on the atmosphere gases. In the O_2/N_2 atmospheres, one has due to Eqs. (4), (10) or (29), (24), and (25),

$$\theta(O_2/N_2;\nabla\delta\neq0) - \theta(O_2/N_2;\nabla\delta=0) = t_{ion}\left\{\frac{\Delta H_i}{2eT}\left[1+\tanh\left(\frac{1}{4}\ln\frac{a_{O_2}}{a^o_{\Delta_2}}\right)\right] - \frac{\Delta H_R}{2eT}\right\} \tag{32}$$

If CO_2/CO atmosphere, then due to Eqs. (4), (10) or (29), (26), and (27) [or due to Eqs. (28)–(30)], one has

$$\rho(CO_2/CO;\nabla\delta\neq0) - \rho(CO_2/CO;\nabla\delta=0) = t_{ion}\left\{\frac{\Delta H_i}{2eT}\left[1+\tanh\left(\frac{1}{4}\ln\frac{a_{O_2}}{a^o_{O_2}}\right)\right] - \frac{\Delta H_R + \Delta H_g^o}{2eT}\right\} \tag{33}$$

As all the values for the defect chemical parameters appearing in Eqs. (30)–(33) are known, both for the "undoped" and Al-doped $BaTiO_3$ [9,11] which will be employed in the present study, one can actually evaluate those thermopower differences.

3. Experimental Procedures

In the present study, two kinds of parallelepiped specimens were employed: one is "undoped" polycrystalline $BaTiO_3$, measuring 2.15mm × 2.15mm × 14.7mm, and the other 1.8m/o Al-doped, single crystal $BaTiO_3$, measuring 1.15mm × 1.15mm × 12mm. These specimens were the same as those upon which both electrical conductivity and chemical diffusivity were previously measured [7–11]. Sample preparation was already detailed elsewhere [6]. Briefly, the polycrystalline sample, with a 94 ± 1% relative density and 43 ± 8 μm grain size, was prepared by sintering a 99.995%-pure $BaTiO_3$ powder (Aldrich, Lot 05717BW). The single crystal sample, with no other appreciable impurities but 1.8 m/o Al, was grown by an exaggerated grain growth technique [25].

Thermocells were constructed into a configuration of Cell (I) as detailed earlier [20]. The measurement set-up is illustrated in Fig. 1. A parallelepiped specimen (⑤ in Fig. 1) was held vertically between the two flattened beads of S-type thermocouples (⑥) with the aid of a piston (④) and cylinder (②) mechanism. A temperature gradient was generated across the specimen by switching on a small heater (⑦), an alumina disk with a fine Pt wire imbedded. This set-up allows one to measure 4-probe electrical total conductivity (σ) and thermoelectric power (θ_{Cell}) simultaneously. Furthermore, the thermopower can, in principle, be measured in the very initial transient state (called a heat pulse technique [20]) where any oxygen nonstoichiometry is yet to redistribute (i.e., $\nabla\delta = 0$), and in the steady state (thus called a steady state technique [20]) where a steady state nonstoichiometry gradient is established (i.e,. $\nabla\delta \neq 0$).

Temperature difference (ΔT) is monitored by the two pairs of thermocouple (⑥ in Fig. 1) and thermovoltage ($\Delta\varphi$) by their Pt legs. The temperature difference imposed along a specimen is controlled by adjusting the dc voltage applied to the heater. Figure 2 shows typical temporal variations of ΔT and $\Delta\varphi$ across the specimen upon switching on and off the heater. It is first noted that there is essentially no time lag between ΔT and $\Delta\varphi$, ensuring both thermal and electrical contact between the thermocouple beads and the specimen to be satisfactory. As is seen, it takes about 300 sec for temperature difference and thermovoltage to apparently achieve the steady state values. In order to evaluate θ_{Cell}, one may replot these variations as $\Delta\varphi$ vs. ΔT with time t as a parameter, which is as shown in Fig. 3. In the very initial transient state or as t→0 upon heating, the specimen will be in the state $\nabla\delta = 0$ because the oxygen nonstoichiometry may not be kinetically redistributed. One can, thus, in principle, determine the thermopower for $\nabla\delta = 0$ as the very initial slope of the plot (as ΔT→0). On the other hand, one may observe that the steady state with respect to nonstoichiometry redistribution (i.e., $\nabla\delta \neq 0$) is

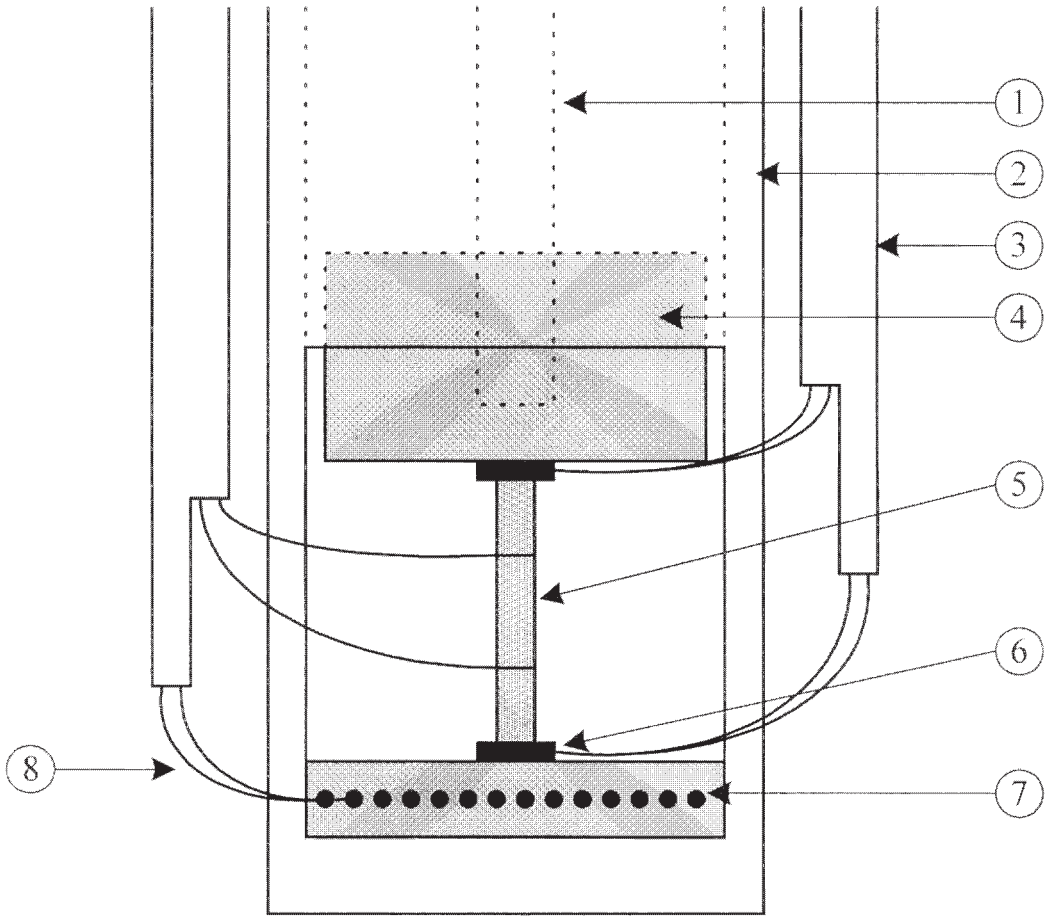

Fig. 1. Schematic of a thermocell. 1, alumina rod pressed by a spring; 2, alumina tubing (cylinder); 3, 4-bore alumina tubing; 4, alumina piston; 5, specimen; 6, S-type thermocouple beads flattened; 7, small resistance heater; 8, Pt lead wires.

achieved as t→ or at the point "A" in Fig. 3, and hence, the steady state thermopower (i.e., for $\nabla\delta \neq 0$) can be determined from a collection of data $\{\Delta T, \Delta\varphi\}$ corresponding to the point "A", exemplified in Fig. 4. It appears, however, in Fig. 4 that all the data fall on a single slope, suggesting that within the present experimental precision, the very initial slope will be hardly discerned from the steady state one. The uncertainty associated with the thermopower turned out to be normally $\pm$ 50 μV/K for the initial transient technique while no greater than $\pm$ 15 μV/K for the steady state technique. (A larger uncertainty with the former technique seems to be attributed to the effect of induction current upon turning on the micro heater and/or the noise from a relay which allows ΔT and $\Delta\varphi$ to be registered alternately by an interfaced personal computer.) As will be shown later, we failed to observe any appreciable difference between the two thermopowers and hence, all the rest of thermopowers were determined by the steady state technique.

The resistance of the micro-heater was ca. 10Ω at 1000°C. The temperature difference imposed upon a specimen was controlled to 9K at maximum and the mean temperature of the specimen was controlled to be within $\pm$ 3K from the temperature of conductivity measurement. Data $\{\Delta T, \Delta\varphi\}$ were collected when the system completely achieved the steady state at each of the 7 different ΔT's imposed (For the present specimens, 5 min after switching on the heater was long enough, see below). The steady state thermopower θ_{Cell} was then determined as the slope of the 7 data, as shown in Fig. 4. The intercept always falls at the ori-

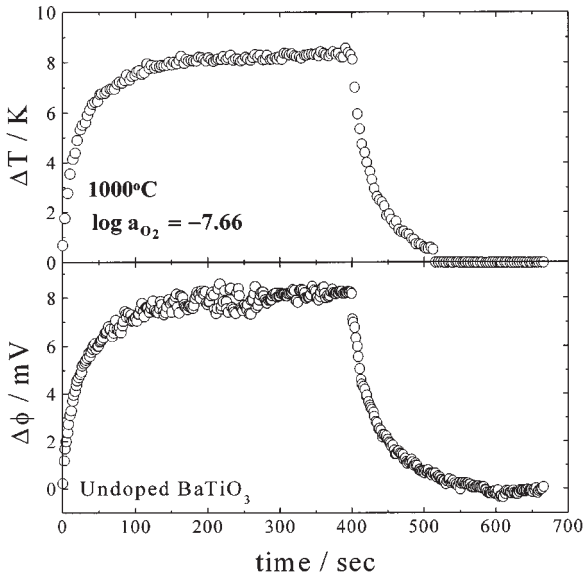

Fig. 2. Typical variation of ΔT and $\Delta\varphi$ with time when a voltage was applied to the local heater and turned off subsequently.

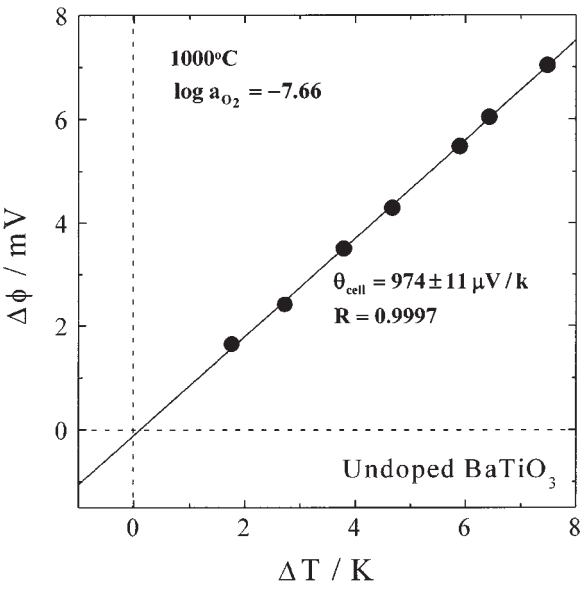

Fig. 4. $\Delta\varphi$ vs. ΔT by a steady state technique. "R" denotes the linear correlation factor.

gin, within experimental error, and the linear correlation coefficient was always greater than 0.999. The absolute thermopower of $BaTiO_3$ was finally evaluated by correcting for the absolute thermopower of the lead wire Pt [26] in accord with Eq. (1).

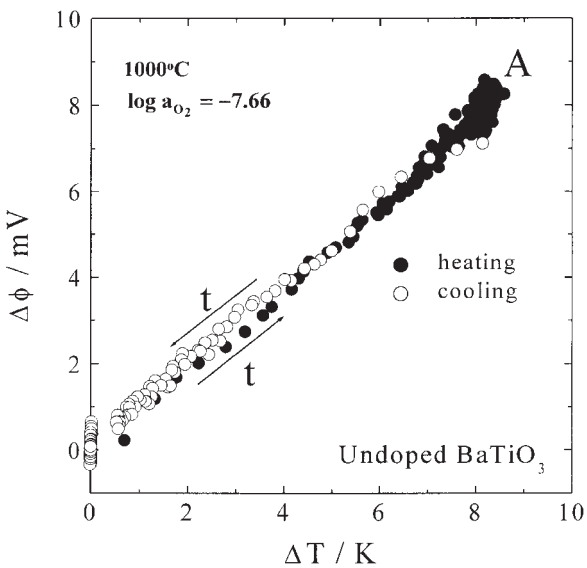

Fig. 3. Replot of Fig. 2 as $\Delta\varphi$ vs. ΔT. "A" represents the datum in the steady state.

Measurements were carried out at 800, 900, 1000, and 1100°C, respectively, versus oxygen partial pressure in the range of $10^{-18} \leq Po_2/atm \leq 1$. The latter was controlled by O_2/N_2 (for $Po_2 > 10^{-5}$ atm, e.g., at 1000°C) and CO_2/CO gas mixtures (for $Po_2 < 10^{-7}$ atm e.g., at 1000°C) and monitored by zirconia-based electrochemical cells.

4. Results

4.1. Electrical Conductivity and Ionic Transference Number

The total conductivities that were measured simultaneously with thermopower are in agreement within less than 1 % with those that have already been reported on the "undoped" and Al-doped $BaTiO_3$, respectively, along with their chemical diffusivities [7–11]. Nevertheless, they are reproduced in Fig. 5 for immediate comparison with the corresponding thermopowers. In the n/p mixed regime, $[A'_C] \approx 2[V_O^{\cdot\cdot}]$, a total conductivity isotherm can be represented as

$$\sigma = \sigma_{el,m} \cosh\left(\frac{1}{4}\ln\frac{a_{O_2}}{a^*_{O_2}}\right) + \sigma_{ion} \qquad (34)$$

which are depicted by the solid lines across the con-

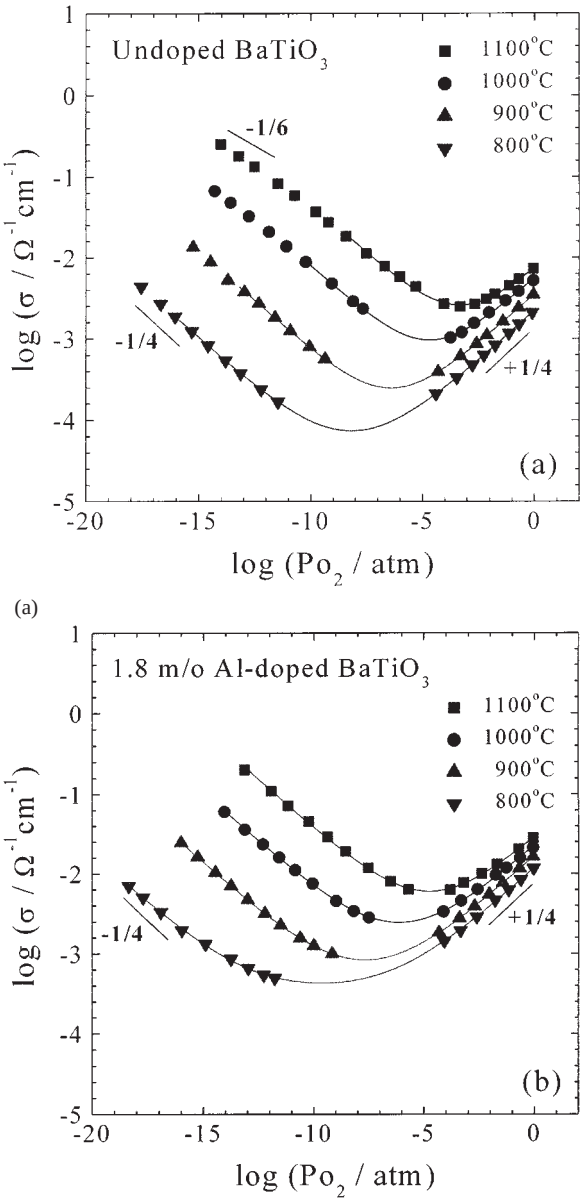

Fig. 5. The isotherms of total electrical conductivity for (a) undoped and (b) 1.8 m/o Al-doped $BaTiO_3$, respectively. The solid lines are the best fitted.

ductivity minima in Figs. 5(a) and (b). As is seen, all the isotherms can be satisfactorily depicted by Eq. (34) over the almost entire Po_2 range examined. The best fitted values for the minimum electronic conductivity, $\sigma_{el,m}$, the partial ionic conductivity, σ_{ion}, and the oxygen activity $a^*_{O_2}$ at $\sigma_{el,m}$ or at $\sigma_n = \sigma_p$ are listed in Tables 1 and 2.

By rearranging Eq. (34), one can evaluate the electronic transference number as shown in Figs. 6(a) and (b), where the solid lines are the best fits. The ionic transference number has maximum values $t_{ion} = 0.464 \sim 0.227$ for undoped $BaTiO_3$ and $0.718 \sim 0.271$ for Al-doped $BaTiO_3$ with increasing temperature from 800° to 1100°C. An ionic contribution to the thermopower is thus highly likely to be seen.

4.2. Thermopower in the Initial Transient and Steady State

The initial transient state technique is, in principle, designed to determine the thermopower for $\nabla\delta = 0$ [20], but its experimental viability hinges on nonstoichiometry reequilibration kinetics of a given system. We have already recognized from Fig. 3 that $\theta(\nabla\delta = 0)$ per se may not be able to be determined because of the fast kinetics of nonstoichiometry redistribution and the lateral boundary of the specimen being left open. Nevertheless, we compare the thermopowers, one determined in the "initial transient state" and the other in the steady state in Fig. 7 for the A1-doped specimen at 900°C as a typical example.

As already expected, the transient state thermopower can hardly be discerned from the steady state counterpart within the experimental error, but one can see that the transient thermopower is consistently larger than its counterpart or

$$\theta(\nabla\delta \neq 0) - \theta(\nabla\delta = 0) < 0. \tag{35}$$

As $\Delta H_i = 2.15$ eV, $\Delta H_R = 5.88$ eV and $\log a^o_{O_2} = -8.35$ (at 900°C) for the 1.8 m/o Al-doped $BaTiO_3$

Table 1. Parameters, $\sigma_{el,m}$, σ_{ion} and $a^*_{O_2}$, evaluated from the isotherms of total electrical conductivity for the undoped $BaTiO_3$.

T/°C	$\log \sigma_{el,m}$ (Ω^{-1} cm^{-1})	$\log \sigma_{ion}$ (Ω^{-1} cm^{-1})	$\log a^*_{O_2}$ ($= P^*_{O_2}$/atm)
800	− (4.401 ± 0.008)	− (4.463 ± 0.089)	− (8.714 ± 0.020)
900	− (3.756 ± 0.008)	− (4.155 ± 0.065)	− (6.400 ± 0.020)
1000	− (3.191 ± 0.010)	− (3.681 ± 0.083)	− (4.772 ± 0.025)
1100	− (2.740 ± 0.015)	− (3.272 ± 0.100)	− (3.447 ± 0.041)

Table 2. Parameters, $\sigma_{el,m}$, σ_{ion} and $a^*_{O_2}$, evaluated from the isotherms of total electrical conductivity for 1.8 m/o Al-Doped $BaTiO_3$.

T/°C	$\log \sigma_{el,m}$ (Ω^{-1} cm^{-1})	$\log \sigma_{ion}$ (Ω^{-1} cm^{-1})	$\log a^*_{O_2}$ (= $P^*_{O_2}$/atm)
800	− (4.032 ± 0.012)	− (3.627 ± 0.075)	− (9.585 ± 0.020)
900	− (3.401 ± 0.007)	− (3.353 ± 0.019)	− (7.631 ± 0.020)
1000	− (2.877 ± 0.005)	− (3.095 ± 0.024)	− (6.060 ± 0.013)
1100	− (2.440±0.003)	− (2.870±0.016)	− (4.659±0.007)

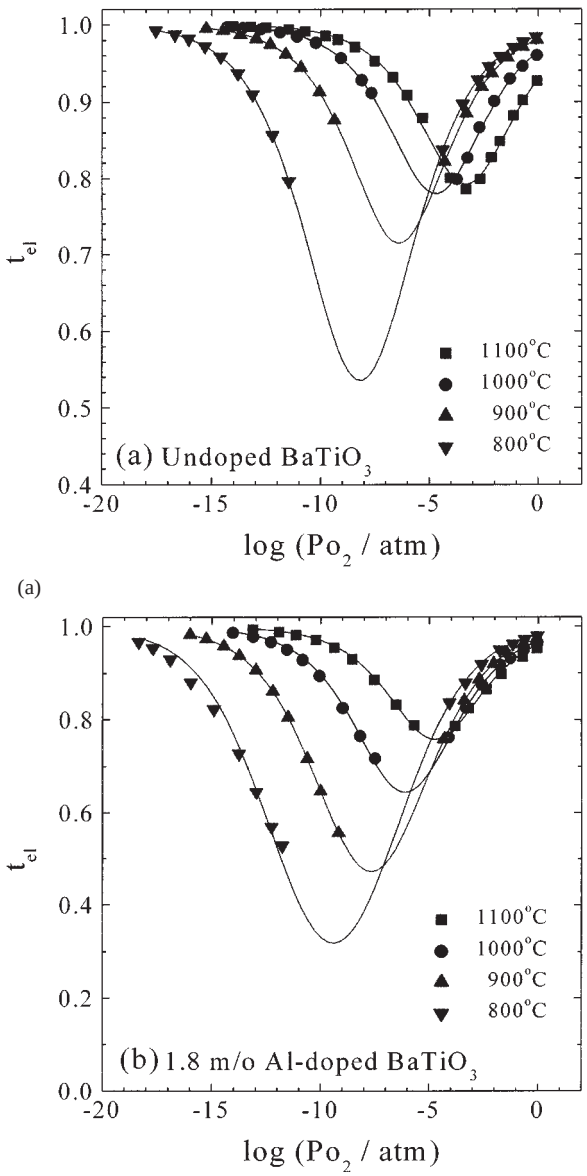

Fig. 6. Electronic transference number, t_{el}, of (a) undoped and (b) 1.8 m/o Al-doped $BaTiO_3$ against oxygen partial pressure. The solid lines are the best fitted.

[11] and $\Delta H^o_g = -2.93$eV, [27] Eq. (32) predicts at $\log a_{O_2} = -4$, where $t_{ion} = 0.20$ (Fig. 6(b)), that $\theta(O_2 / N_2; \nabla\delta \neq 0) - \theta(O_2 / N_2; \nabla\delta = 0) = -137\,\mu$V/K, and Eq. (33) predicts at $\log a_{O_2} = -9$, where $t_{ion} = 0.25$ that $\theta(CO_2 / CO; \nabla\delta \neq 0) - \theta(CO_2 / CO; \nabla\delta = 0) = -99.5\,\mu$V/K. The negative sign of the difference in Eq. (35) is in accord with the prediction, but as seen in Fig. 7, the magnitude obtained is far smaller than predicted. Considering the error associated with the thermopower difference is ± 50μV/K, the expected difference of 100∼140 μV/K should have been detected if the nonstoichiometry redistribution had been kinetically suppressed during measurement in the initial transient state so that $\nabla\delta = 0$.

It is, however, highly likely that the nonstoichiometry redistribution was already occurring even during measurement. We have known [10,11] that the surface reaction rate constant and chemical diffusion

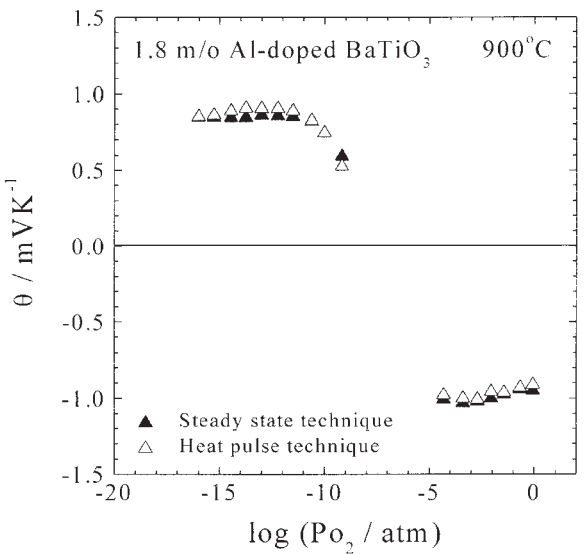

Fig. 7. Themopower of 1.8 m/o Al-doped $BaTiO_3$ against oxygen partial pressure measured by the heat pulse and steady state techniques, respectively, at 900°C.

coefficient for the system are $\kappa/\text{cms}^{-1} \geq 3.5 \times 10^{-4}$ and $\tilde{D}/\text{cm}^2\text{s}^{-1} \geq 6.3 \times 10^{-5}$, respectively, over the entire range of Po_2 examined at 900°C for the Al-doped specimen. If the lateral boundary of the parallelepiped specimen had been closed and hence, the redistribution proceeded only in the longitudinal axis ($2c = 1.2$ cm, see Experimental) of the specimen, the relaxation time would have been $\tau \leq 1700$ sec and 2300 sec when the overall kinetics were controlled by the surface reaction ($\tau = c/\kappa$) and the diffusion ($\tau = 4c^2/\pi^2\tilde{D}$), respectively [10,11]. In reality, however, the lateral boundary along the longitudinal axis was left open and, hence, the redistribution would likely have taken place laterally across the cross section of $4a^2 = 0.115 \times 0.115$ cm^2. In this case, $\tau \leq 82$ ($= a/2\kappa$) and 11 ($= 2a^2/\pi^2\tilde{D}$) sec, respectively [8,11].

Therefore, the condition of $\nabla\delta = 0$ could hardly have been realized with the present measurement technique and 5 minutes were long enough for the crystal to achieve the steady state. Nevertheless, this steady state cannot be a Soret equilibrium but one that is locally in equilibrium with the immediate surrounding along the longitudinal axis.

4.3. Thermopower in the Steady State

The steady state, absolute thermopowers as determined from Cell (I) are shown in Figs. 8(a) and (b) for the "undoped" and Al-doped $BaTiO_3$, respectively. It should be recalled that the data in the range of $\log(Po_2/\text{atm}) < -5$ were obtained in CO_2/CO atmospheres and the rest (in the range of $\log(Po_2/\text{atm}) > -5$) in O_2/N_2 atmospheres. As demonstrated by the conductivity isotherms in Fig. 5, almost the entire range of Po_2 examined is enclosed in the defect regime of $[A'_C] \approx [V_O^{\cdot\cdot}]$. One can immediately recognize that the isotherms, particularly of the Al-doped specimen, deviate from anti-symmetry and the deviation becomes more appreciable as temperature is lowered. If the specimen were purely electronic or $t_{el} >> t_{ion}$, the isothermal variation of absolute thermopower against $\log a_{O_2}$ would be anti-symmetric as indicated by Eq. (29). This deviation from the anti-symmetry, or a dependence on measurement atmospheres, clearly indicates that the ionic contribution is appreciable to the thermopower of $BaTiO_3$.

The thermopowers as measured in CO_2/CO atmospheres are normalized to that of O_2/N_2 atmospheres via Eq. (31) by using the values for t_{ion} as determined in Fig. 2 or Tables 1 and 2. The results are as shown in Figs. 9(a) and (b).

The normalized thermopower may be represented by associating Eqs. (25) and (29) via Eq. (4) as

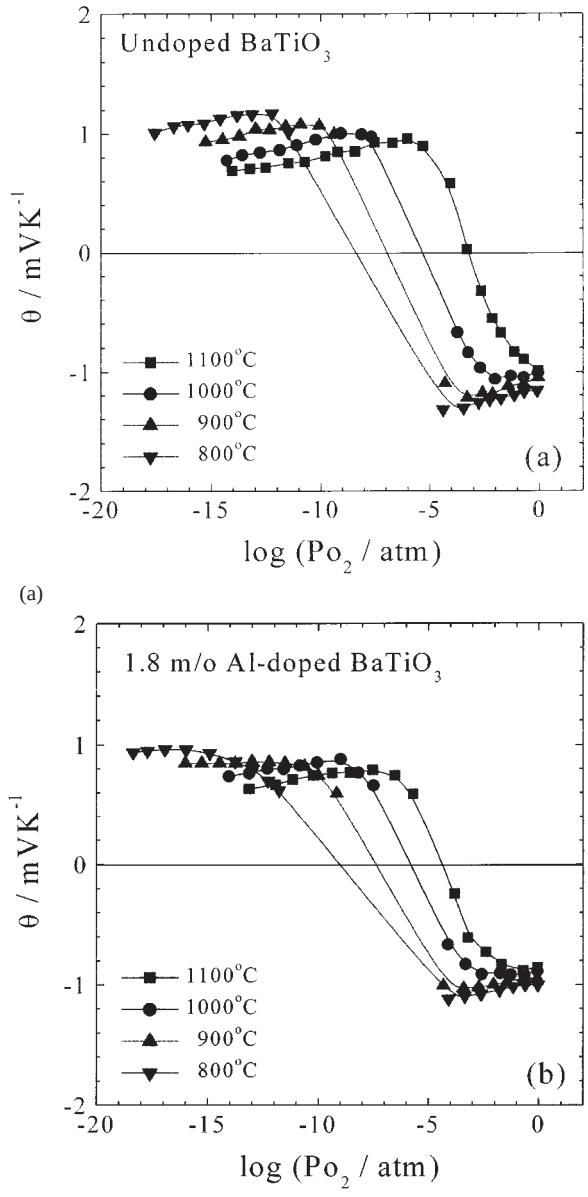

Fig. 8. As-measured isotherms of steady state thermopower of (a) undoped and (b) 1.8 m/o Al-doped $BaTiO_3$, respectively. The solid lines are for visual guidance only.

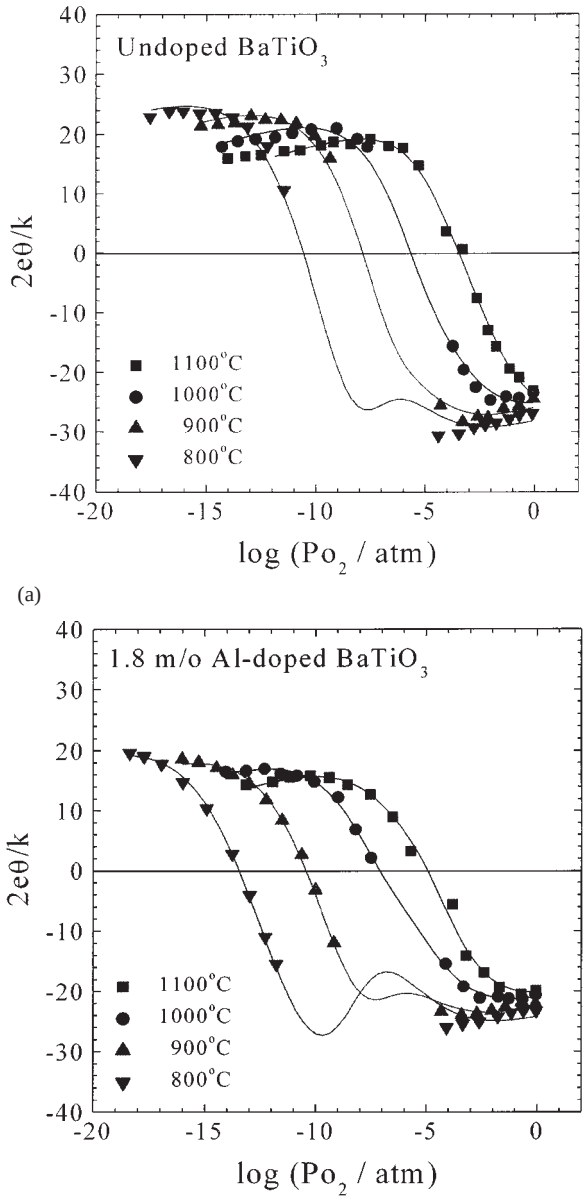

Fig. 9. Normalized thermopower isotherms of (a) undoped and (b) 1.8 m/o Al-doped $BaTiO_3$, respectively. The solid lines are the best fitted. See text for description

$$\frac{2e\rho}{k} = t_{ion}\left\{A + B\left[1 + \tanh\left(\frac{1}{4}\ln\frac{a_{O_2}}{a^{o}_{O_2}}\right)\right] + \frac{1}{2}\ln a_{O_2}\right\}$$
$$-t_{el}\left[C\tanh\left(\frac{1}{4}\ln\frac{a_{O_2}}{a^{*}_{O_2}}\right) - \frac{1}{2}\ln\frac{a_{O_2}}{a^{*}_{O_2}} - \ln b + D\right] \qquad (36)$$

where

$$A = -\frac{S^{o}_{O_2}}{2k} + \frac{\bar{S}_{O^{2-}}}{k} + \frac{q^{*}_{O^{2-}}}{kT} - \frac{\Delta H_R}{kT}\ ;\ B = \frac{\Delta H_i}{kT}\ ;$$
$$C = \frac{\Delta H_i + q^{*}_{p} + q^{*}_{n}}{kT};\ D = \frac{q^{*}_{p} - q^{*}_{n}}{kT} + \frac{\bar{S}^{o}_{p} - \bar{S}^{o}_{n}}{k} \qquad (37)$$

We have previously evaluated $t_{ion}(= 1-t_{el})$, $a^{o}_{O_2}$, $a^{*}_{O_2}$, b, and ΔH_i (hence B) from the isothermal conductivities and chemical diffusivities of the same specimens at each temperature. [9,11] By using these values and assuming that the parameters A, C and D are insensitive to oxygen activity, we fit the normalized thermopower isotherms to Eq. (36). The results are as depicted by the solid lines in Fig. 9 and the fitting parameters A, C and D are evaluated as listed in Tables 3 and 4. One may see that Eq. (36) reasonably well explains the isotherms. It is noted that the ionic thermopower is expected to become more conspicuous, particularly in the vicinity of $a^{o}_{O_2}$ at the stoichiometric composition, as the temperature is lowered, say at 900 and 800°C. These ionic humps are due to the W-factor increasing as a_{O_2} increases beyond $a^{o}_{O_2}$, and t_{ion} becoming a maximum at $a^{*}_{O_2}$ which is close to $a^{o}_{O_2}$. Unfortunately, however, the actual observation could not be made because this oxygen partial pressure region was normally hard to realize experimentally. As a consequence any further quantitative analysis of the ionic thermopower cannot be made from the fitted values for A, and the attention is drawn to the electronic part.

Table 3. Parameters, A, C and D, evaluated from the isotherms of normalized thermopower for the undoped $BaTiO_3$.

T/°C	A	C	D
800	− (59.0 ± 6.2)	36.86 ± 0.40	2.46 ± 0.57
900	− (68.2 ± 5.9)	33.19 ± 0.33	1.14 ± 0.47
1000	− (48.0 ± 5.4)	31.01 ± 0.44	1.72 ± 0.57
1100	− (5.0 ± 3.2)	30.45 ± 0.37	4.59 ± 0.50

Table 4. Parameters, A, C and D, evaluated from the isotherms of normalized thermopower for 1.8 m/o A1-doped $BaTiO_3$.

T/°C	A	C	D
800	− (33.4 ± 1.5)	33.82 ± 0.37	3.83 ± 0.43
900	− (43.1 ± 1.4)	30.32 ± 0.22	2.28 ± 0.29
1000	− (30.3 ± 1.4)	27.46 ± 0.15	1.14 ± 0.21
1100	− (26.8 ± 3.5)	25.52 ± 0.41	0.35 ± 0.54

4.4. Transported Entropies of Electronic Carriers

As the absolute thermopower in Fig. 9 is mostly governed by the electronic contribution, the evaluated values for the electronic parameters C and D may be regarded as relatively more reliable. One may first take the difference "C-B" in Tables 3 and 4 to evaluate the sum of the heats of transport, $q_p^* + q_n^*$ at each temperature, which turns out to be temperature-insensitive and is best estimated as

$$q_p^* + q_n^* = 0.26 \pm 0.11 eV \quad \text{for the undoped } BaTiO_3 \tag{38a}$$

$$0.91 \pm 0.06 \text{ eV for the Al-doped } BaTiO_3 \tag{38b}$$

It is noted that the value for the doped specimen, 0.91 eV, is conspicuously larger than for the undoped $BaTiO_3$. Assuming that the standard entropies of electronic carriers, $\overline{S}_p^o$ and $\overline{S}_n^o$, are insensitive to temperature, one may plot the parameter D against reciprocal temperature to determine the difference of the heats of transport. The results are as shown in Fig. 10. The variation of D for the undoped specimen is in general quite different from that of the doped sample, but the partial trend below 900°C looks quite similar to that of the doped sample. A rationale for this behavior comes from the prior study on electrical conductivity and chemical diffusivity [9,11] which strongly suggested that the defect structure of the same undoped specimen is of intrinsic origin and is frozen-in upon passing 900°C, and hence the trend of the properties of the undoped specimen appear the same as that of the Al-doped below 900°C. However, the nature of defect structure of the undoped $BaTiO_3$ still remains to be elucidated. Therefore we will further analyze only the result for the doped specimen.

Unlike the undoped specimen, the variation of D vs. reciprocal temperature is highly linear for the Al-doped sample, as expected from Eq. (37), with the values for the slope and intercept as

$$q_p^* - q_n^* = 1.48 \pm 0.08 eV \;;\; \overline{S}_p^o - \overline{S}_n^o = -(1.06 \pm 0.06) \times 10^{-3} eV/K \tag{39}$$

One thus obtains from Eqs. (38b) and (39),

$$q_p^* = 1.20 \pm 0.05 eV \;;\; q_n^* = -0.29 \pm 0.05 eV \tag{40}$$

The heat of transport of holes has turned out to be much larger than that of electrons, which is close to zero. Surprisingly, these values are very close to the activation energies of mobility of holes and electrons for the doped specimen, which are respectively, 1.14 ± 0.02 eV and − (0.2 ± 0.1) eV. [11] The nature of the heat of transport remains still unknown, [19] nevertheless Tan [28] has recently proposed that if the effect of a thermal gradient on the solubility and segregation of a species *i* is negligible, its heat of transport should be the same as the migration enthalpy of the species or

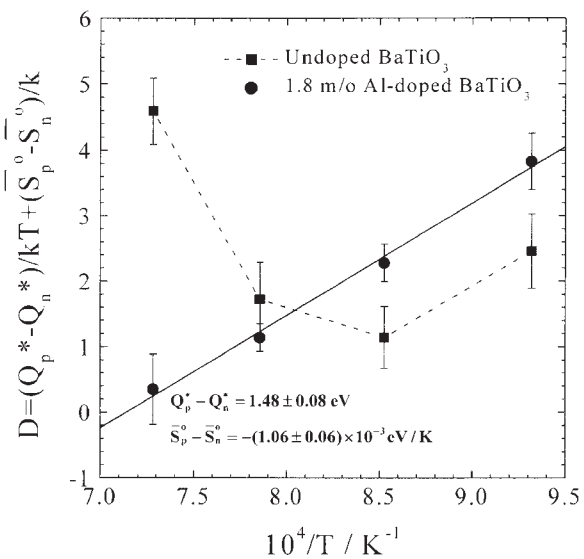

Fig. 10. The fitting parameter D against reciprocal temperature for undoped and 1.8 m/o Al-doped $BaTiO_3$. The solid line is the best fit.

$$q_i^* = \Delta H_{m,i} \tag{41}$$

$$q_i^* = \Delta H_{m,i} \quad (41)$$

For the undoped $BaTiO_3$, [9] it has been found that the mobilities of holes and electrons are insensitive to temperature at temperatures of $\geq 900°C$, where the intrinsic nature of the defect structure is suggested. Then, $q_p^* + q_n^* \approx 0$ in the light of Eq. (41), which is in agreement with the present result, Eq. (38a). It thus seems that the present results support the validity of Eq. (41).

Another result in Eq. (39) indicates that $\overline{S}_n^0 > \overline{S}_p^0$, which in turn points to $m_n^* > m_p^*$ according to the modified Sackur-Tetrode equation. [18,29] It is reported on $BaTiO_3$ [15,30–34] that $3.9 \leq m_n^* / m_o \leq 7.5$, but little is reported on m_p^*. For $SrTiO_3$, however, the effective mass of heavy holes has been calculated to be $m_p^* / m_o < 3$. [35] Considering the structural and chemical similarity of $SrTiO_3$ and $BaTiO_3$, the present result seems to be in agreement.

5. Conclusions

In conclusion, there can be four possible conditions of thermopower measurement of $BaTiO_{3+\delta}$ depending on the distributions of δ (i.e., $\nabla\delta = 0$ or $\nabla\delta \neq 0$) and on the types of gas mixtures to control the surrounding oxygen activity (e.g., CO_2/CO or O_2/inert gas mixtures). Thermoelectric information contents are accordingly different unless the ionic contribution is negligible. It has been found that in the n/p mixed regime of $BaTiO_3$, the ionic contribution to thermopower is appreciable at the temperature range examined. The reduced heats of transport of electrons and holes are $q_p^* = 1.2$eV and $q_n^* \approx 0$, respectively, for 1.8 m/o Al-doped $BaTiO_3$ and $q_p^* + q_n^* \approx 0$ for undoped $BaTiO_3$. These values appear to be the same as the migration enthalpies of holes and electrons for the doped and undoped materials, respectively, which supports a recent proposal [28] that the reduced heat of transport of a species be equal to the migration enthalpy of the species. It is therefore warned that the evaluation of electronic carrier concentration from thermopower is likely to lead to an erroneous conclusion, particularly when the system is extrinsically doped, without paying a due attention to the possible ionic contribution and the non-negligible heat-of-transport of electronic carriers.

Acknowledgements

One of the authors (HIY) gratefully acknowledges the generous support of Prof. J. Mizusaki for his research stay at the Research Institute for Scientific Measurements, Tohoku University, Japan during which this work has been completed. This work was partially supported by the Alexander von Humboldt Foundation, Germany.

List of Symbols

a,c, dimensions of parallelepiped specimens
a_{O_2}, activity of gas oxygen ($\equiv P_{O_2}/atm$)
$a_{O_2}^o$, oxygen activity where $n = p$
$a_{O_2}^*$, oxygen activity where $\sigma_n = \sigma_p$
b, electrochemical mobility ratio of electrons to holes
$\tilde{D}$, chemical diffusion coefficient
e, fundamental charge
$\overline{H}_k$, partial molar enthalpy of species k
i_k, partial current density by species k
i_n, partial current by free electrons
i_p, partial current by electron holes
k, Boltzmann constant
K_i, intrinsic electronic excitation equilibrium constant
$K_{i,0}$, pre-exponential factor of K_i
K_R, reduction equilibrium constant
$K_{R,0}$, pre-exponential factor of K_R
m_n^*, effective mass of free electrons
m_p^*, effective mass of electron holes
m_o, rest mass of electrons
n, density of free electrons
N_A, Avogadro's number
p, density of electron holes
P_{CO}, partial pressure of CO
P_{CO_2}, partial pressure of CO_2
P_{O_2}, oxygen partial pressure
q_k^*, reduced heat of transport of species k
r, mixing ratio CO_2 to CO ($= P_{CO_2}/P_{CO}$)
$\overline{S}_k$, partial molar entropy of species k
$\overline{S}_k^o$, standard partial molar entropy of species k (k = n,p)
$S_{O_{2(g)}}^o$, standard entropy of gas oxygen
T, absolute temperature (K)
t_{el}, electronic transference number
t_{ion}, ionic transference number ($= 1 - t_{el}$)
u_k, electrochemical mobility of species k
V_m, molar volume of $BaTiO_3$
z_k, valence of species k

∇, gradient operator
a, hole to electron conductivity ratio
δ, oxygen excess or nonstoichiometry of $BaTiO_{3+\delta}$
ΔH_g^o, standard enthalpy of the reaction $CO + \frac{1}{2} O_2 = CO_2$
ΔH_i, enthalpy of intrinsic electronic excitation reaction (= thermal band gap)
$\Delta H_{m,k}$, migration enthalpy of species k
ΔH_R, enthalpy of reduction reaction
ΔT, temperature increment
$\Delta\varphi$, electrical potential increment
η_{el}, electrochemical potential of electrons as a charged component
θ, absolute thermoelectric power of $BaTiO_3$
θ_{Cell}, thermopower of a thermocell as a whole
θ_{el}, thermopower by charged component electrons
θ_{ion}, thermopower by mobile ions
θ_{Pt}, absolute thermopower of metal Pt
κ, surface reaction rate constant
μ_k, chemical potential of species k
ξ, nonmolecularity such as $Ba_{1+\xi}TiO_{3+\delta}$
σ, total conductivity
$\sigma_{el,m}$, minimum electronic conductivity
σ_k, partial conductivity of species k
τ, relaxation time
Indices (k)
O, neutral oxygen as a neutral component
O^{2-}, oxide ion as a charged component
ion, ion as a mobile charged component (= O^{2-} in the present context)
el, electron as a mobile charged component
n, carrier electrons
p, carrier holes

References

1. E.K. Chang, A. Metha, and D.M. Smyth, in *Proceedings of the Symposium on Electro-Ceramics and Solid State Ionics*, H.L. Tuller and D.M. Smyth, eds. (The Electrochemical Soc., Princeton, NJ, 1988), p. 35.
2. A.Z. Heb and D.S. Tannhauser, *J. Chem. Phys.*, **47,** 2090 (1967).
3. J. Yahia, *Phys. Rev.*, **130,** 1711 (1963).
4. J. Nowotny, M. Radecka, and M. Rekas, *J. Phys. Chem. Solids*, **58,** 927 (1997).
5. J. Nowotny and M. Rekas, *Solid State Ionics*, **49,** 135 (1991).
6. J.-Y. Kim, C.-R. Song, and H.-I. Yoo, *J. Electroceram.*, **1,** 27 (1997).
7. C.-R. Song and H.-I. Yoo, in *Solid State Ionics: Science & Technology*, B.V.R. Chowdari et al., eds. (World Scientific Publishing Co., Singapore, 1998), p. 149.
8. C.-R. Song and H.-I. Yoo, *Solid State Ionics*, **120,** 141 (1999).
9. C.-R. Song and H.-I. Yoo, *Phys. Rev. B*, **61,** 3975 (2000).
10. C.-R. Song and H.-I. Yoo, *Solid State Ionics*, **124,** 289 (1999).
11. C.-R. Song and H.-I. Yoo, *J. Am. Ceram. Soc.*, **83,** 773 (2000).
12. C. R. Song and H.-I. Yoo, to be published.
13. P. Gerthsen, R. Groth, and K.H. Härdtl, *Phys. Stat. Sol.*, **11,** 303 (1965).
14. A.M.J.H. Seuter, *Phil. Res. Repts. Supply.*, **3,** 1 (1974).
15. G.M. Choi, H.L. Tuller, and D. Goldschmidt, *Phys. Rev. B*, **34,** 6972 (1986).
16. G.M. Choi and H.L. Tuller, *J. Am. Ceram. Soc.*, **71,** 201 (1988).
17. J. Nowotny and M. Rekas, *Ceram. Int.*, **20,** 225 (1994).
18. C. Wagner, *Prog. Solid State Chem.*, **7,** 1 (1972).
19. C. Jones, P.J. Grout, and A.B. Lidiard, *Phil. Mag. A*, **79,** 2051 (1999).
20. H.-I. Yoo and J.-H. Hwang, *J. Phys. Chem. Solids*, **53,** 973 (1992).
21. J.H. Becker and H.P.R. Frederickse, *J. Appl. Phys. Suppl.*, **33,** 447 (1962).
22. G.H. Jonker, *Phil. Res. Repts.*, **23,** 131, (1968).
23. H.-I. Yoo, D.-S. Sinn, and J.-O. Hong, *J. Electrochem. Soc.*, **145,** 1008 (1998).
24. S.R. de Groot, *Thermodynamics of Irreversible Processes* (North-Holland, Amsterdam, 1951).
25. Y.-S. Yoo, M.-K. Kang, J.-H. Han, and D.-Y. Kim, *J. Eur. Ceram. Soc.*, **17,** 1725 (1997).
26. N. Cusack and P. Kendall, *Proc. Phys. Soc. (London)*, **72,** 898 (1958).
27. D.R. Gaskell, in *Introduction to the Thermodynamics of Materials, 3rd ed.* (Taylor & Francis, Washington, DC, 1995), p. 329.
28. T.Y. Tan, *Appl. Phys. Lett.*, **73,** 2678 (1998).
29. G.S. Rushbrooke, in *Introduction to Statistical Mechanics* (Clarendon Press, Oxford, 1949), p. 47.
30. M. DiDomenico, Jr. and S.H. Wemple, *Phys. Rev.*, **166,** 565 (1968).
31. H. Ihrig, *J. Phys. C*, **9,** 3469 (1976).
32. C.N. Berglund and W.A. Baer, *Phys. Rev.*, **157,** 358 (1966).
33. J.P. Boyeaux and F.M. Michel-Calendini, *J. Phys. C*, **12,** 545–56 (1979).
34. E. Iguchi, N. Kubota, T. Nakamori, and K.J. Lee, *Phys. Rev. B*, **43,** 8646 (1991).
35. A.H. Kahn and A.J. Levendecker, *Phys. Rev.*, **135,** 1321 (1964).